NIAC Swarm Flyby Gravimetry
Phase II Report

Fellow: Dr. Justin A. Atchison

       The Johns Hopkins University Applied Physics Laboratory

       Justin.Atchison@jhuapl.edu

       (443) 778-1488

       11100 Johns Hopkins Road

       Laurel, MD 20723

Research Team:

       Dr. Ryan Mitch

       Clint Apland

       Calvin Kee

       Dr. Andy Rivkin

       Dr. Erwan Mazarico

       Ken Harclerode

       Jake Wortman

       Kyle Candela

Contents

1   Abstract

This NASA Innovative Advanced Concept (NIAC) grant has enabled the research and development of a method for conducting small body gravimetry from a spacecraft, using relative measurements to a set of deployed test-masses. The test-masses are tracked from a host spacecraft, which dispenses them near to the small body's surface. Thanks to this close proximity, the probes' orbits can be highly perturbed, which yields useful gravimetric measurements. The most readily achievable approach for tracking the probes is to use an optical instrument on-board the spacecraft. The probes then need only be reflective to sunlight. This implementation, called optical gravimetry (OpGrav), has the fewest requirements for the host spacecraft and probes.

The results of this study indicate that OpGrav is feasible and offers meaningful improvement over existing methods. Parametric studies suggest roughly an order of magnitude improvement in accuracy or asteroid accessibility (how small an asteroid one can measure) over Earth-based Doppler-only mass estimation. This exponentially expands the number of potential near-Earth objects that one could study, which has implications for planetary defense.

As a sample mission, we evaluated OpGrav as an added instrument on a main-belt asteroid tour mission. In this case, simulations show that OpGrav would increase the number of asteroid mass estimates from 3 of 9 to 7 of 9. That is, OpGrav has sufficient sensitivity to offer utility in missions for which it is not explicitly designed for.

We designed and fabricated a prototype hardware implementation for this concept called the Small-body In-situ Multi-probe Mass Estimation Experiment (SIMMEE). This hardware provides a basis for many inputs into the simulations and grounds the models with physical values. The primary design driver for the hardware is a long life, on the order of five years prior to operation, and a need for high pointing accuracy to enable flybys of the smallest objects.

The next steps include further hardware testing and extension of the concept to rendezvous cases. We believe that this concept offers planetary scientists a new and relevant means of better understanding small-bodies.

2   Introduction

2.1   Context

Asteroid and comet gravimetry, and the subsequent density and porosity estimates derived from gravimetry, are relevant to space-science, planetary defense, and future human spaceflight. Scientifically, it has implications for the formation models of our solar system. Consolmagno, Britt, and Macke[1] suggest that small body density and porosity can give important insights into the early solar system's accretional and collisional environment. For planetary defense, an asteroid's porosity has implications for its potential impact risk as well as the appropriate mitigation technique[2]. Finally, asteroid density and porosity are relevant for human spaceflight since near-Earth objects are often considered as targets for human exploration and in-situ resource utilization. Material density and porosity relate to handling, anchoring, or landing approaches that one might pursue.

A body's mass is typically observed by measuring its effect on the trajectory of a smaller neighbor, such as a moon or spacecraft[3]. That is, by tracking the moon or spacecraft's change in motion, one can estimate properties of the object's gravitational field. The observability of the field depends principally on the strength of the field being measured and the quantity, geometric diversity, and accuracy of the measurements. For small bodies, these measurements are difficult to obtain. Few asteroids have companions that can be tracked, so we generally have to rely on observations of spacecraft. This is achieved by launching and maneuvering a spacecraft to fly past, orbit, or land on a small body while tracking the spacecraft from the ground. While orbiters and landers offer the highest quality science, they require dedicated missions and are often constrained to a single target due to practical limitations of spacecraft capabilities (e.g. propellant).

Flybys are favorable because they are often easily added to existing mission designs with little impact to cost or operations; however, they present many challenges for gravimetry. Flybys are typically short-lived events owing to relative velocities of many kilometers per second. The magnitude of deflection from an asteroid is a function of the mass of the asteroid, the asteroid-spacecraft relative velocity, and close approach range to the center-of-mass. For typical relative velocities (5-15 km/s) the spacecraft must pass very close to the asteroid to achieve a measurable deflection. The high relative velocity implies a short-time-duration conjunction and the asteroid exerts only a weak gravitational force that diminishes in proportion to r^{-2}. The close proximity can represent a risk or at least operational

challenge to the mission. In addition, low-altitude passes may degrade the science from other instruments that cannot accommodate the high spacecraft slew rates required to track the small-body during a close pass (e.g., cameras or spectrometers).

2.2   Concept

This work seeks to conduct gravimetry via flyby despite these challenges, by having the host spacecraft deploy and track small spherical test-masses that we call probes. The host spacecraft can fly by the small body at a distance optimized for long-range science (e.g. narrow-angle cameras), while the probes enable close-proximity or in-situ gravity science. The gravimetric measurements are then conducted using radiometric tracking of the host spacecraft from Earth and relative measurements of the probes from the host spacecraft[4]. Figure 1 depicts a notional sequence of events. The probes are dispensed prior to the flyby with roughly 3-5 m/s of separation from the host spacecraft. The probes then drift very close to the asteroid. The whole ensemble flies past the asteroid typically with velocities of many kilometers per second. Since gravitational acceleration is proportional to r^{-2}, the probes may experience an observable variation in their heliocentric orbit. Multiple probes can be used to obtain additional and unique measurements.

The most readily achievable approach for tracking the probes is to use an optical instrument on-board the spacecraft. The probes then need only be reflective to sunlight. The imager locates the probes with respect to the star-background, such that it downlinks a time-history of measurements of right ascension and declination. This implementation, called optical gravimetry (OpGrav), has the fewest requirements for the host spacecraft and probes. From Earth, the angular change in the probes' trajectories would be essentially unmeasurable, but the short range between the host and the probes enables the measurement.

We've developed a hardware implementation of OpGrav called the Small-body In-situ Multi-probe Mass Estimation Experiment (SIMMEE). It consists of a dispenser that efficiently houses and accurately ejects multiple probes. Although other versions (e.g. Doppler only) and applications (e.g. rendezvous scenarios) of this concept are likely realizable, this phase of the research and hardware development focuses on flybys using optical only measurements.
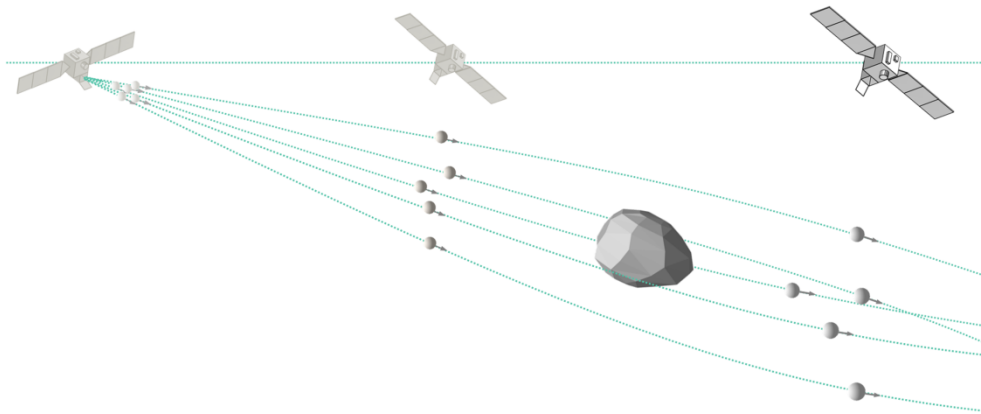
Figure 1. OpGrav concept of operations: A set of probes is deployed from a host spacecraft prior to a flyby. The relative motion of each probe is tracked by the host spacecraft and used to determine the asteroid's mass.

A nominal OpGrav concept-of-operations is similar to existing flyby science approaches. The experiment requires a long time-series of probe relative measurements (i.e. images against the star background) prior to the flyby and following the flyby. This is compatible with and similar to the requirements for optical navigation (OpNav). However, during the few hours of operations surrounding close-approach, the gravimetry experiment can be ignored. That is, it need not interfere with close-approach activities like asteroid imaging or spectroscopy. In the spans of time when the probes are being imaged, it is desirable for the host spacecraft to be in contact with the ground with radiometric tracking. The experiment benefits from frequent images of the probes, e.g. 2 images per minute. The ensemble of probes doesn't spread to a large angular extent, so any spacecraft slews are small, albeit potentially frequent.

A representative timeline is illustrated in Figure 2. Once the flyby and tracking campaign is complete, all of the data is downlinked to the science team on the ground. Then, the typical estimation results are generated using radiometric and optical measurements: spacecraft ephemeris, small-body shape model, and spin-state. Following these results, the relative measurements to the probes are processed to compute the mass of the small-body. Then, given a small-body mass and volume, we can compute the mean density. If the science suite is able to identify the composition of the small-body, e.g. using spectroscopy, we can also derive a mean porosity. As is typical of flyby operations, the spacecraft would flyby the small-body on its sunlit side. This benefits the close approach science, as well as maximizing the visibility of the dispensed probes. The dispenser direction

can be varied somewhat to target different locations where the probes flyby, while still ensuring positive lighting conditions. The target locations of each probe's flyby is a relatively complicated trade-study, but involves dispenser accuracy, pre-flyby asteroid knowledge, and observability of the change in probe trajectory. Dispensing multiple probes increases the diversity of the measurements while also improving the likelihood of achieving a favorable probe flyby condition, in spite of unavoidable uncertainties.
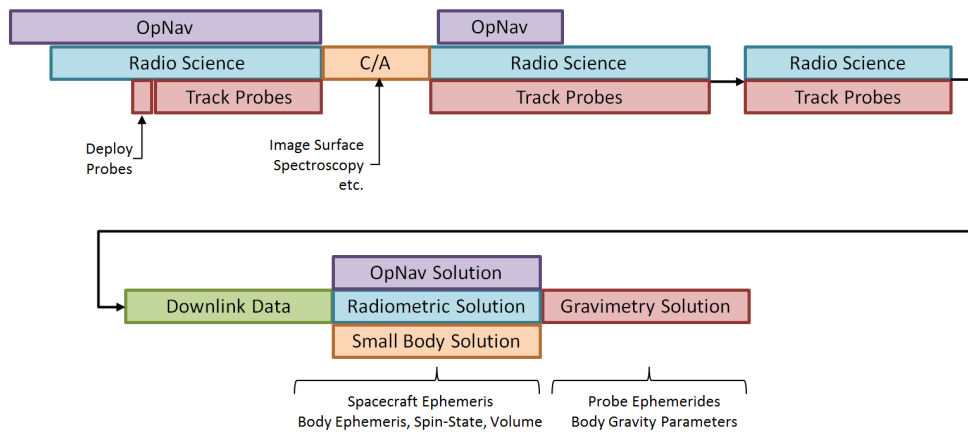

Figure 2. Representative OpGrav flyby operations timeline

3   Modeling and Simulation

This concept can only be assessed prior to flight using modeling and simulation. This includes mathematical models for the acceleration environment (dynamics), the statistically optimal estimators, and the observations. Given the dependence on modeling, we conducted a validation study against a flight-proven, independent software tool. Once validated, our simulations are used to determine OpGrav's performance in different flight concepts and scenarios.

3.1   Dynamics Models

The environmental accelerations, or dynamics models, are used in truth simulations and optionally in the estimator. We implemented the following dynamics models, including partial derivatives: point-mass gravity, analytical J2 gravity, arbitrary spherical harmonics, tetrahedral plate-model gravity, solar radiation pressure, and N-body gravity (gravity associated with planets or moons that are not the model's central body). Based on the time-scales of an OpGrav scenario, this fidelity is sufficient to discriminate beteween the desired small-body gravity field and natural environmental perturbations.

3.2   Estimators

Three different estimators were implemented for this research: a recursive batch-least-squares (BLS) [5], an extended square-root information filter (SRIF), and an unscented Kalman filter (UKF). In previous parametric studies, the numerical performance of the filter was a limiting factor. The SRIF has the advantage of being numerically well-behaved. It also allows for the inclusion of process noise, which acknowledges the limitations of our dynamics models. The UKF is a means of reducing the impact of nonlinearities on the problem. In combination, these three approaches gave us means of assessing our solutions and gaining confidence in results.

3.3   Tracking

The probes are intended to be tracked optically using a preexisting imager on-board the spacecraft. That is, SIMMEE ought not require a dedicated imager for most small-body spacecraft designs. Table 1 evaluates a set of flight-heritage spacecraft telescopes: the LOng-Range Reconnaissance Imager (LORRI)[6] instrument flown on New Horizons, the Mercury Dual Imaging System - Narrow Angle Camera (MDIS-NAC)[7] flown on MESSENGER, and the Framing Camera

8

(FC)[8] flown on the Dawn Spacecraft. One key output is the probe detection range, which was evaluated with 45° lighting for a 1.0 second integration time. The probe and its material reflectivity properties are described in greater detail in Section 4.3. The detection range dictates how long the probes can be tracked, given that they're drifting away from the host spacecraft. For a typical dispenser speed of 4 m/s, a detection range of 1000 km corresponds to roughly 3 days of tracking. The second key parameter is the instantaneous field-of-view (iFOV) which dictates the accuracy of each measurement. We conservatively assume that we can centroid down to 1/4 of a pixel. Given that the imager captures both the probe and stars in its field-of-view (FOV), spacecraft platform accuracy is not a driver. The values given in Table 1 suggest that all of the telescopes have utility for OpGrav, though LORRI is the highest performing, owing to its large aperture and narrow FOV. The downside to using LORRI is that its narrow FOV may require multiple pointing directions to fully image the ensemble of multiple deployed probes.

Table 1. Simulated Telescope Tracking Performance

Parameter	LORRI	MDIS-NAC	Dawn-FC
FOV, deg	0.29 x 0.29	1.05 x 1.05	2.93 x 2.25
Number of Pixels	1024 x 1024	1024 x 1024	537 x 244
iFOV, arcsec	1.0	5.15	19.3
Aperture Area, cm^2	339.8	4.62	3.41
Bandwidth, nm	350-850	725-775	450-920
Probe Tracking Range at 45° Phase, km	7700	300	800
Angular Accuracy, arcsec	0.25	1.3	4.8

3.4　Validation

We worked with Dr. Mazarico to validate our models against NASA's GEODYN software. This software has extensive flight-use for gravity field estimation in Earth[9], Lunar[10], Martian[11], and small-body[12] regimes. It uses a batch-least-squares estimator. GEODYN does not currently have the capability to simulate an OpGrav encounter, at least not directly. In order to validate the modeling and simulation environments, we chose instead to evaluate a test scenario using radiometric Doppler tracking.

In this case, we both modelled a hypothetical spacecraft passing Eros, a small S type body with an 8.42 km equivalent radius. In the scenario (Figure 3), the spacecraft departs Earth on May 2022 and flies past Eros on 12 May 2024 with a relative velocity of 6.94 km/s. Earth based observatories use Doppler tracking to estimate the spacecraft's state relative to Eros, as well as the point-mass gravity of Eros.

This process highlighted differing approaches within the software. After aligning all of the input statistics, the final GM estimate means agree to less than 5% and standard deviations agree to less than 15% over the convergence region. These results are presented in Figure 4. Additional samples (random draws on initial parameters) show similar behavior.
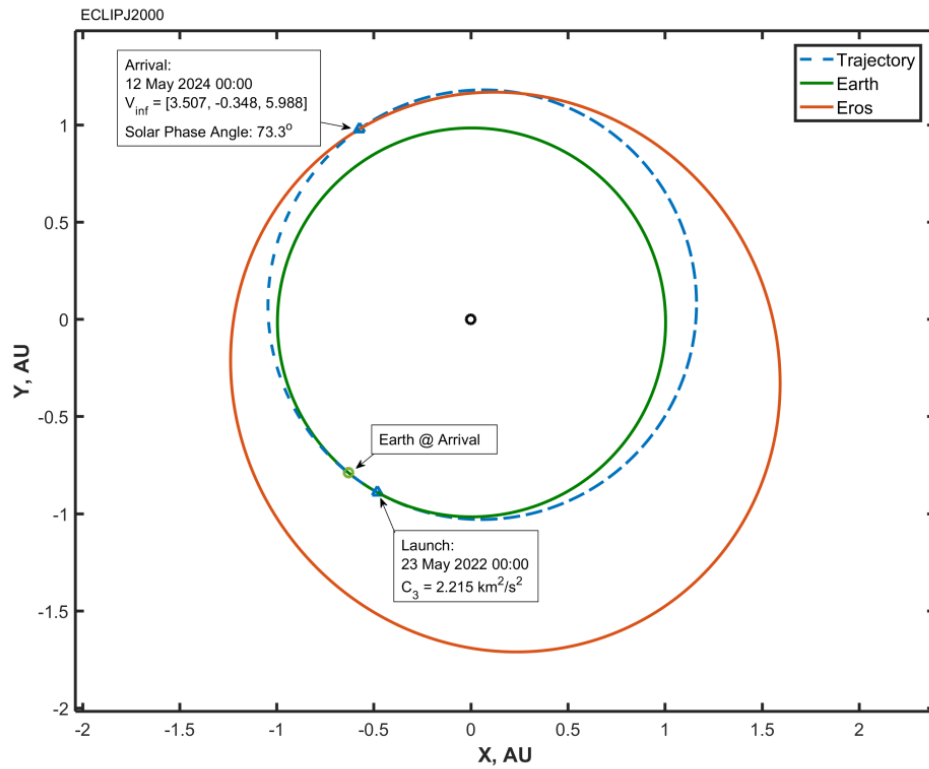

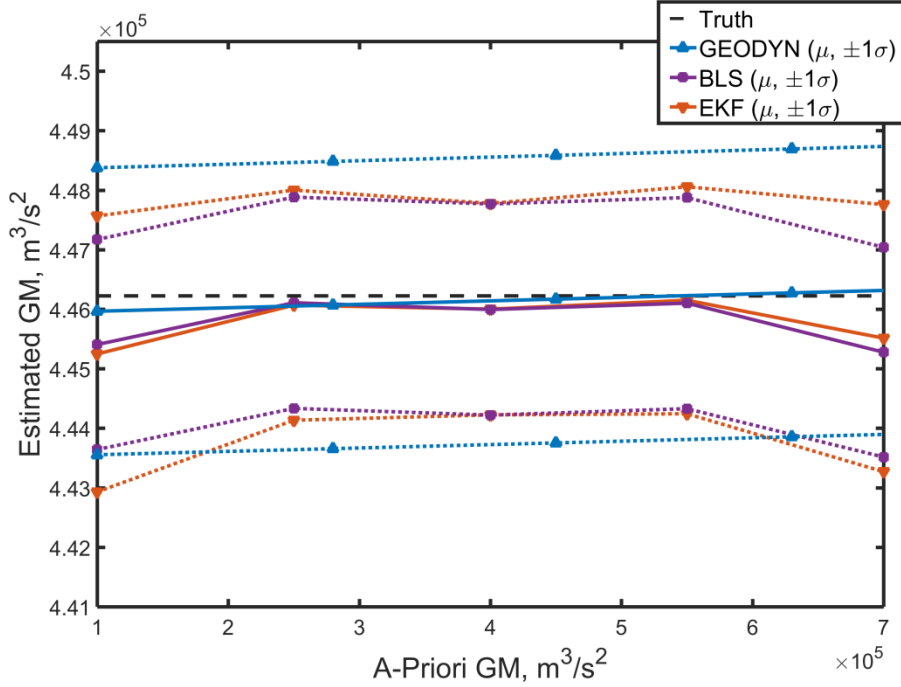Figure 3. Hypothetical Eros flyby example used to compare our models with GEODYN. The trajectory of the spacecraft is depicted in ecliptic coordinates.

Figure 4. Doppler tracking validation results for GEODYN and for the OpGrav modeling environment using batch-least-squares (BLS) and an extended Kalman filter (EKF). The final estimated point-mass value for Eros is plotted over varying initial a-priori initial estimates.

3.5   Parametric Results

The hypothetical Eros flyby geometry described in Section 3.4 served as the basis for a parametric study [13]. We considered three different small-body sizes (radius of 0.5, 1.0, and 2.5 km) and four different flyby velocities (2.5, 5.0, 7.5, and 10.0 km/s) to determine the ranges at which OpGrav can return useful results. We evaluated sets of 200 Monte-Carlo cases using OpGrav instead of Doppler tracking. In each case, 3 probes are deployed prior to the flyby and tracked using an imager similar to the New Horizons LORRI telescope. The asteroid is assumed to be S type with a mean density of 2.0 g/cm^3.

The plots give the 10th (bottom), 50th (middle), and 90th (top) percentile results for each set of Monte-Carlo runs. These results show meaningful improvements to Doppler-only gravimetry, enabling mass estimation for smaller (1 km radius) asteroids, or increasing accuracy for larger asteroids. For very small asteroids (0.5 km radius), high quality estimates are still possible. The performance is heavily dependent on the achieved probe flyby distance. This motivates a hardware prototype to better understand what deployment accuracy is achievable.
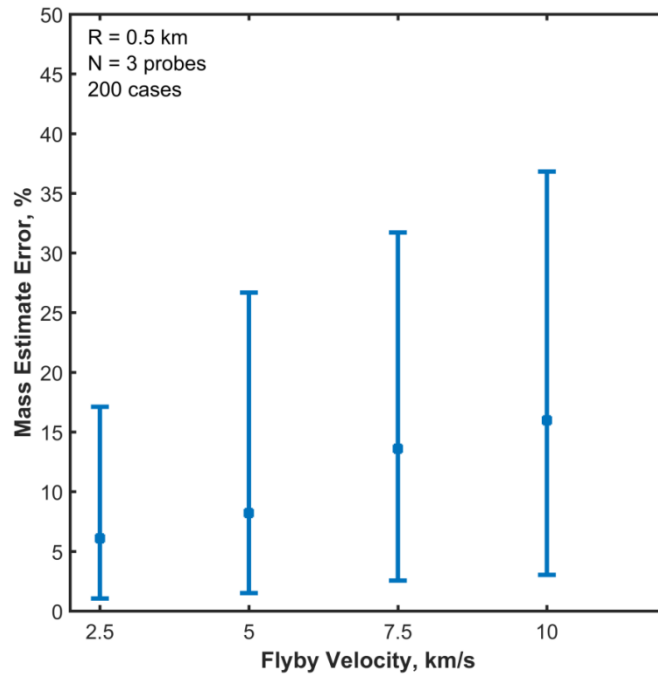
11

Figure 5. Point-Mass Monte-Carlo OpGrav results for a 0.5 km radius small-body. Lines correspond to 10th (bottom), 50th (middle), and 90th (top) percentile results.
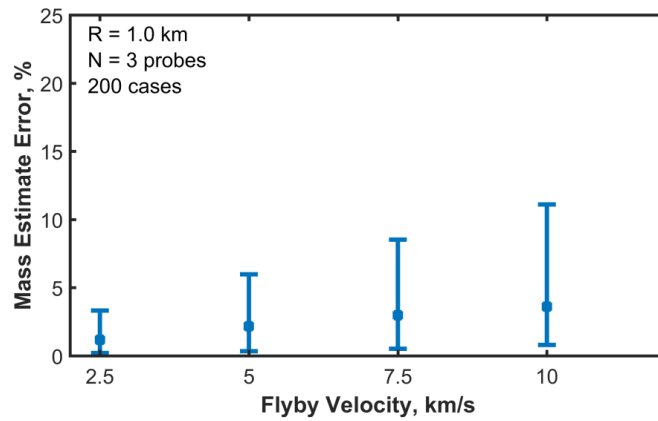

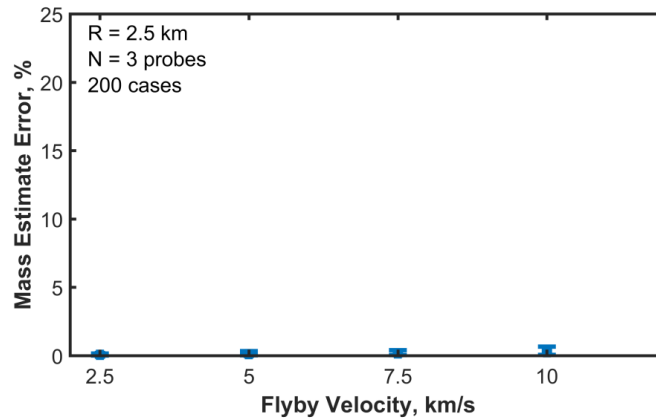Figure 6. Point-Mass Monte-Carlo OpGrav results for 1.0 km radius body.

Figure 7. Point-Mass Monte-Carlo OpGrav results for a 2.5 km radius body.

3.6   Planetary Defense

The above parametric results were mapped to the Near-Earth Object (NEO) population to assess OpGrav's applicability to planetary defense studies[14]. The parametric results are a function of small-body size and flyby velocity. The size distribution of NEOs[15] is shown in Figure 8. The number of small objects increases exponentially, implying that even a marginal improvement in gravimetric performance can significantly increase the number of observable objects. To determine a reasonable distribution of flyby velocities, we computed the minimum energy, phase-free transfer from Earth to each NEO in the Minor Planet Center database (Figure 9). This represents the lowest energy transfer to each asteroid from Earth. This distribution is then generalized to the full population, which includes bodies that have not yet been observed.

The mean performance (50%) from the parametric results is then extrapolated to this population model, as shown in Figure 10. This reasonably assumes that NEO size and flyby velocity are uncorrelated. A set of NEO populations were drawn using the above distributions and input into the interpolation model underlying Figure 10. This process was repeated until the results converged. The results are given in Figure 11 and indicate that OpGrav could increase the available set of NEO targets that could be studied by flyby by roughly an order of magnitude.
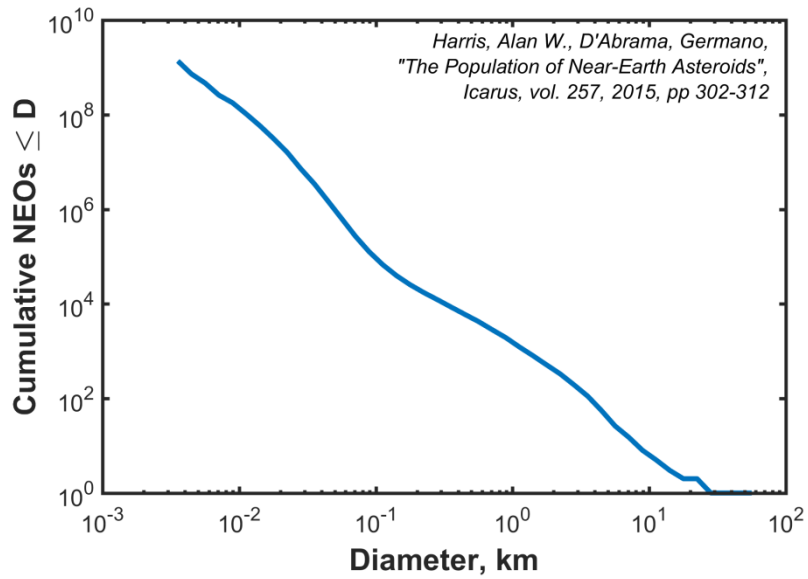
13

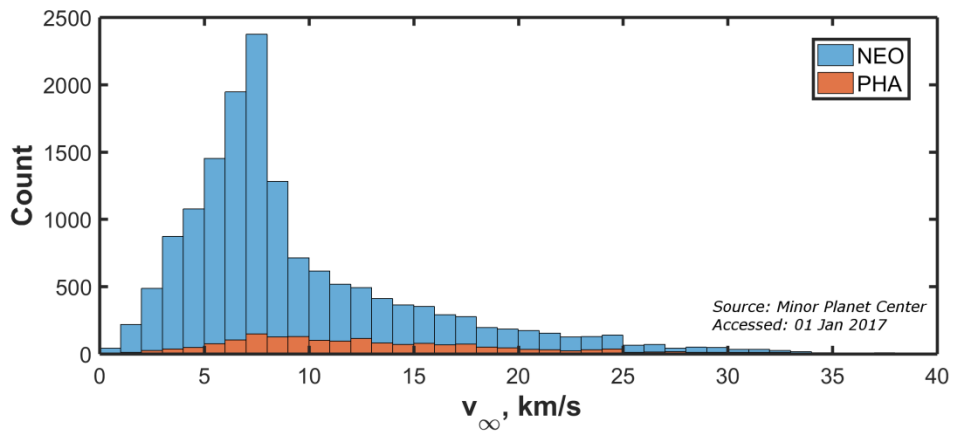Figure 8. Size distribution of Near Earth Objects.

Figure 9. Computed distribution of optimal arrival velocities to known Near Earth Objects and Potentially Hazardous Objects (PHA).
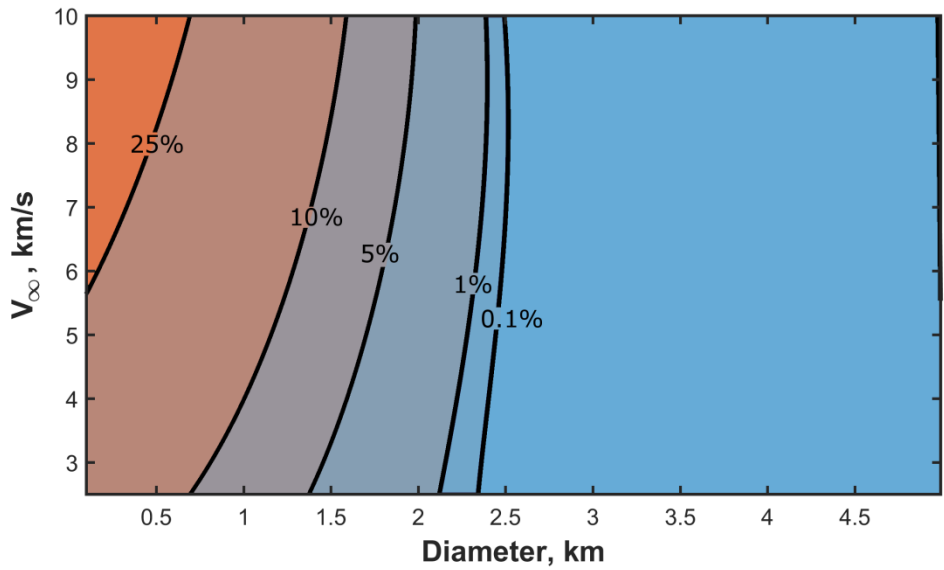
Figure 10. Extrapolated values of OpGrav 50th percentile accuracy as a function of flyby velocity and small-body diameter.
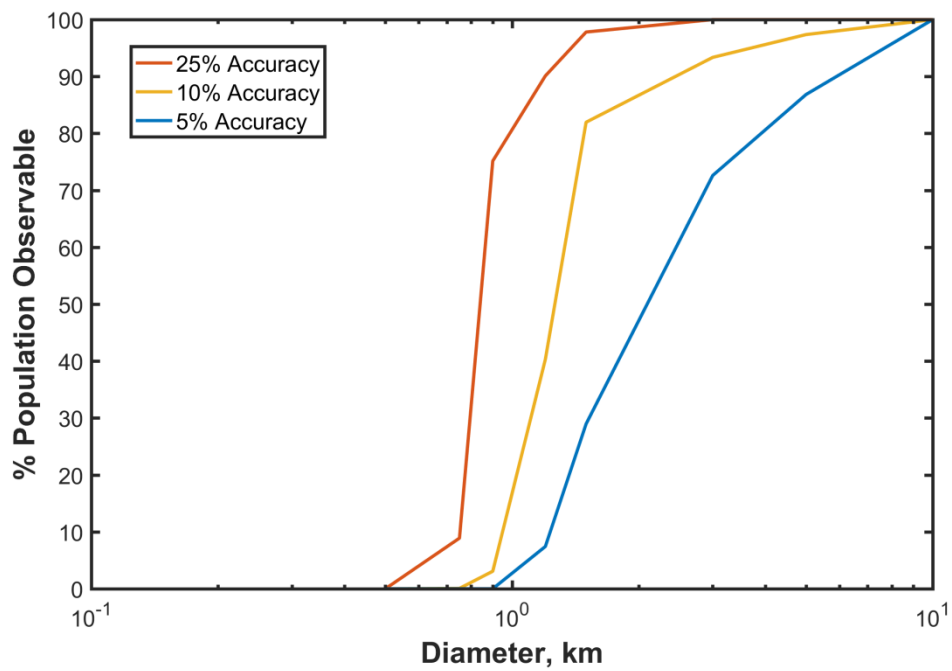

Figure 11. Computed fraction of the population of NEOs of a given size that are observable to a given median accuracy using OpGrav.

3.7   Mission Scenario

OpGrav was evaluated in the context of a Main-Belt asteroid tour [16]. Specifically, we considered its performance as an added instrument on the Mainbelt Asteroid and NEO Tour with Imaging and Spectroscopy (MANTIS) [17], which was submitted to the NASA Discovery Mission-13 Program. The mission as proposed in 2015 consists of 9 flyby events (Table 2) and includes a narrow angle camera, a hyperspectral imager, an infrared imager, a dust instrument, and radio-science. The mission goals included investigations of com-position, geophysics, internal structure, and morphology of its targets. MANTIS would have already acquired mass information for 3 of the bodies: Rutherfordia via radio-science, and 1996 FG3 and 2003 SS84 by measuring those binary system's period and separation. In these cases, OpGrav would either not be used, or would have represented additional measurements used for higher precision or independent validation.

For this simulation, we included N-body gravity and solar radiation pressure in 200 Monte-Carlo simulations. The simulations used a targeted spacecraft flyby point of 100 km in the sunward direction, which is consistent with other instrument needs. The OpGrav test-masses were deployed 12 hours prior to close-approach (C/A) and were targeted to have a nominal fly-by point scaled to 2-σ of the expected uncertainty at the time of C/A. This uncertainty is modeled, such that the true flyby point of a given test-mass is randomly drawn. The results are given in Figure 12 and Figure 13.

Table 2. MANTIS Flyby Parameters

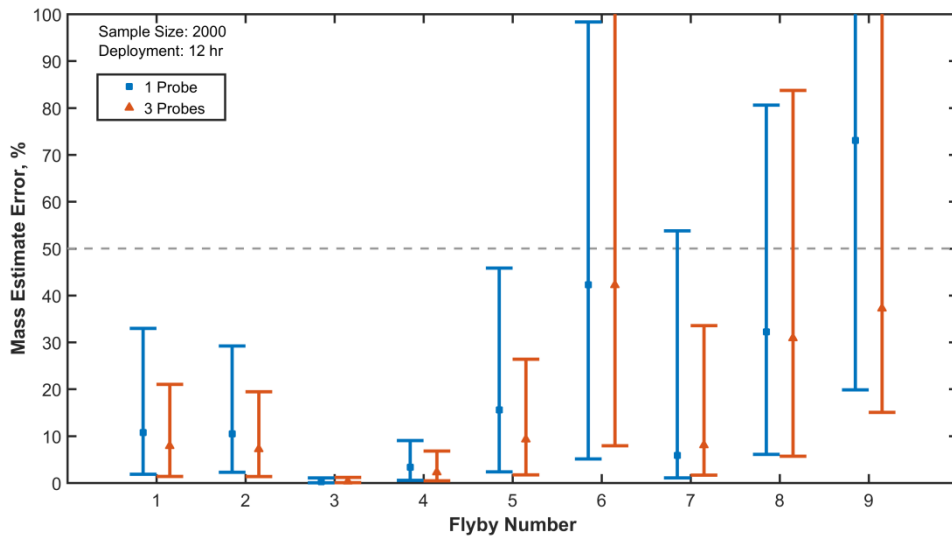| #	Body	Class	Estimated Diameter (km)	Flyby Velocity (km/s)
1	2001 TS3	Unk	1.3	5.9
2	2003 UV185	S	1.2	4.8
3*	Rutherfordia	S	14	5.1
4	Takoyaki	S	3.8	11.0
5*	1996 FG3	C	1.8, 0.45	9.4
6	2012 CD29	Unk	0.45	10.2
7	Amun	X(M)	2.5	12.4
8*	2003 SS84	Unk	0.12, 0.06	21.2
9	2006 XT3	Unk	0.8	8.2

* Mass estimate expected without OpGrav

Figure 12. Percent error of point-mass estimate, based on Monte-Carlo OpGrav results for each MANTIS flyby. Markers correspond to 10th (bottom), 50th (middle), and 90th (top) percentile results. The initial uncertainty of 50% is shown as a horizontal dashed line.
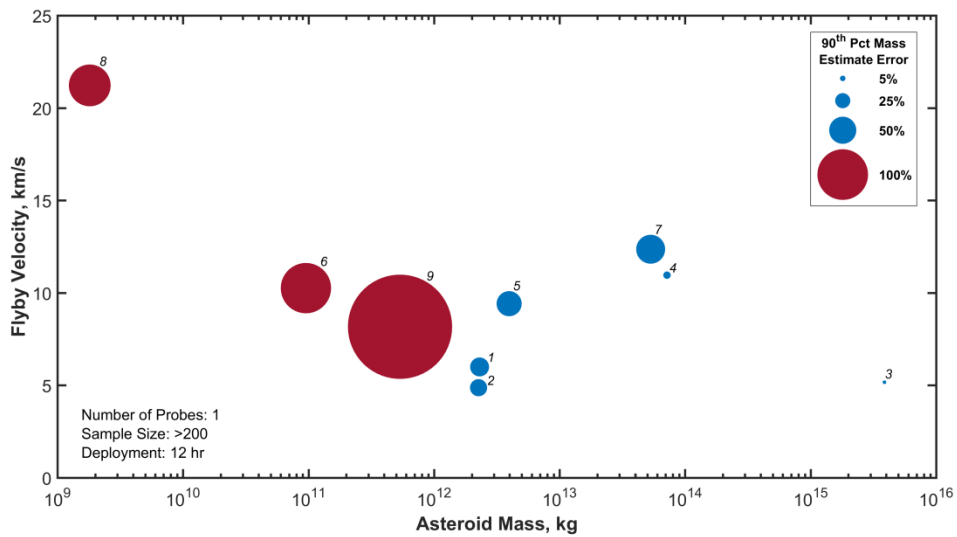

Figure 13. 90th Percentile error of point-mass estimate for each flyby, shown as a function of flyby velocity and asteroid mass. Slower flybys of massive objects give better performance.

17

Based on this analysis, we would seek to implement a 12-probe concept. Our modelled allocation use of these probes, and the associated median performance, is given in Table 3. In summary, OpGrav, if added to the MANTIS mission, would provide useful mass estimates for 4 additional asteroids. In total, MANTIS would achieve a mass estimate for 7 of 9 targets.

Table 3. Notional allocation of 12 probes for MANTIS mission

#	Body	Number of Probes	Median Performance (% Err)
1	2001 TS3	2	9%
2	2003 UV185	3	7%
3*	Rutherfordia	1	<1%
4	Takoyaki	1	3%
5*	1996 FG3	1	16%
6	2012 CD29	0	-
7	Amun	3	8%
8*	2003 SS84	0	-
9	2006 XT3	0	-

4 Prototype Development

4.1 Design Overview

The modeling and simulation results motivated hardware prototype development. A prototype grounds the simulations by providing feasible input values where necessary and points to an eventual flight implementation. Our design of the hardware for OpGrav is called 'Small Body In-Situ Multi-Probe Mass Estimation Experiment' (SIMMEE) [18]. The SIMMEE hardware consists of three components: the set of *probes*, which are housed in *sabots*, and are ejected from a *dispenser*.

4.2 Design Requirements

A hardware implementation of the OpGrav concept must satisfy a set of challenging requirements to be compatible with a generic interplanetary spacecraft bus. The most notable requirement is a functional design life of 5^+ years, which is associated with typical small body asteroid tour mission concepts.

The environmental requirements are defined as:
- Vibration Environment
    - Sine: 36 g in each of 3 orthogonal axes
    - Random: 14.1 g RMS in each of 3 orthogonal axes
- Thermal Environment:
    - Survival Range: -70°C to 65°C
    - Operational Range : -40°C to 65°C
- Radiation:
    - Notionally, components should survive 100 krad behind 2.54 mm (0.1 inch) aluminum with radiation design margin (RDM) of 2 (TBR).

The key functional requirements and objectives are defined as:
- The probe shall use a diffuse, high reflectivity material whose optical properties have minimal degradation from beginning-of-life to end-of-life.
- The probe and dispenser shall function after an unattended period of storage of 5 years in a space environment.
- The probe diameter shall be 150 mm (~6 in), when deployed and minimize volume when stowed.
- The probe center-of-mass and center-of-pressure offset should be very small.

19

The probe ejection shall meet the following accuracy requirements:
- Velocity shall be in the range of 3-5 m/s.
- Velocity repeatability shall be 10 mm/sec or less.
- Azimuth and elevation vector shall be within 0.3 degrees from intended axis (half-angle).
- The probe and dispenser shall meet the following outgassing requirements:
- Materials shall have outgassing total-mass-loss (TML) less than or equal to 1%.
- Materials shall have outgassing collected volatile condensable material (CVCM) less than 0.1%.
- Probe and dispenser shall minimize the use of magnetically permeable materials.

4.3   Probe and Sabot Design

The probe is dispensed and tracked throughout the flyby encounter. It serves as a test-mass, which is perturbed by the asteroid's gravity. We selected a spherical shape so that its optical signature is constant in spite of any induced spin. The spherical shape also simplifies solar-radiation-pressure modeling, which is a disturbance to the experiment.

The probe is a 150 mm (~6 inch) diameter sphere that has an outer surface made of pliable cloth. It can be collapsed into a 150 mm (~6 inch) diameter, 44.5 mm (1.75 inch) thick "puck" with the goal of reducing packaging volume and aid in its ejection into its intended trajectory. The Probe expands from a puck to a sphere using compression springs and a series of stepped disks to guide, synchronize and give form to the soft-goods outer shell (Figure 14). The stepped disks' extent of travel is controlled through a series of aramid tethers. While in the dispenser, the probes are housed in sabots, which ensure that the cloth outer material doesn't interfere with the deployment.

The probe's sabot-to-sphere deployment mechanism consists of a multi-stage, linear compression spring system that has sufficient spring stiffness and deflection at every stage to apply the force on the aluminium inter-stage disks to give shape to the outer shell. Compared to a single spring system, the multi-stage mechanism works better to prevent spring buckling and ensure a spherical shape.
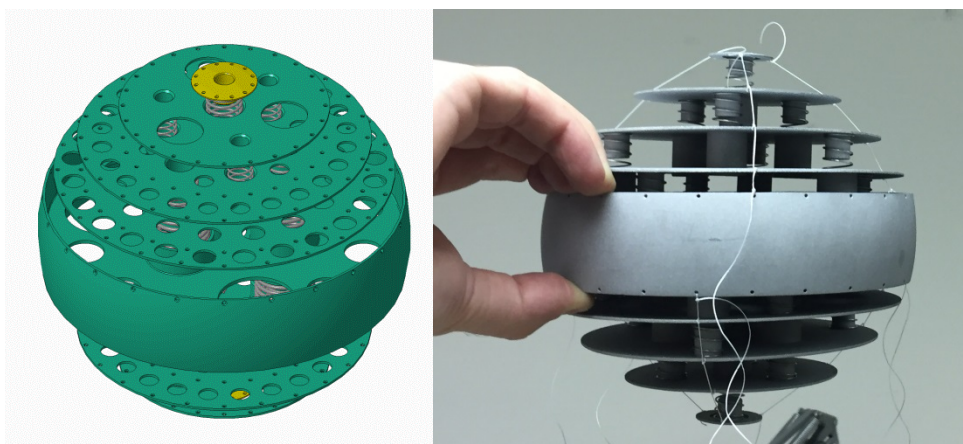
Figure 14. Deployed probe sphere. Drawing at left and photo at right. Thin tethers prevent the probe from overextending while uncovered.

The sabot is a protective canister that helps stow the probe. It also provides radiation shielding. The sabot's exterior is rigid, smooth, and flat to provide repeatable ejection of the probe from the dispenser. It's coated in dicronite to reduce friction with the dispenser. It separates into two identical halves after ejection, leaving the vicinity of the probe (Figure 15). Each half of the sabot has four guide pins and holes. These pins ensure that the halves stay together when in the stowed configuration, and that they separate in parallel without locking up when the sabot exits the dispenser.
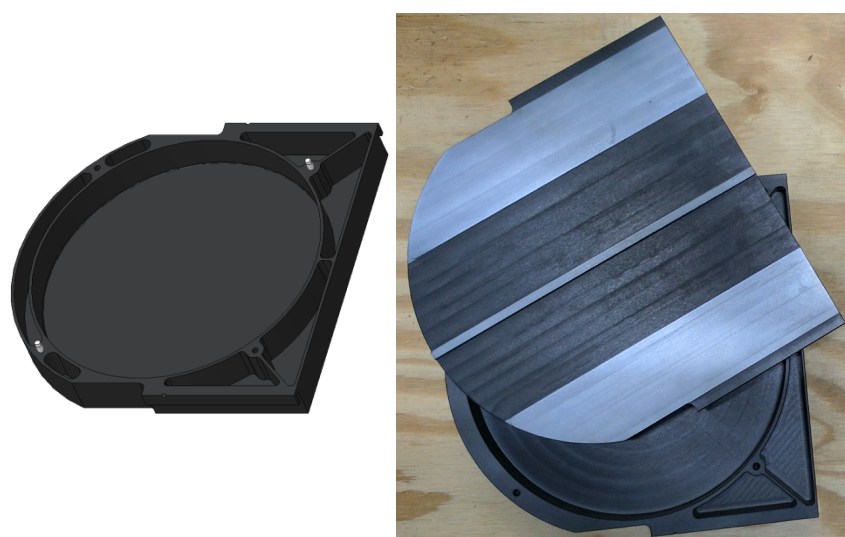
Figure 15. Sabot. Drawing at left and photo at right. A ridge guide in the middle prevents the deployment from jamming.
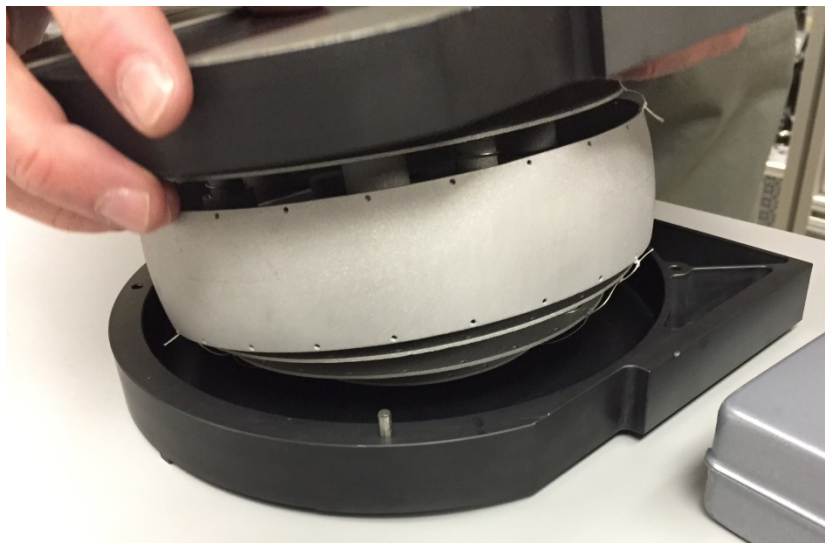
Figure 16. Sabot shell with half-compressed probe sphere inside. Pins (seen at bottom) keep the sabot aligned while deploying.

A key question in the probe design is the selection of an appropriately reflective, operationally suitable material. The material must efficiently reflect sunlight from a variety of lighting angles, while also being pliable over a long duration of time in vacuum. Figure 17 shows a ray-tracing simulation of various space-rated materials applied to the probe design and evaluated at 3.5 AU. It turns out that the two key parameters are the albedo, or total reflectance, and the fraction of reflectance that is diffuse rather than specular. This second component is displayed in Figure 18, which shows the same materials evaluated at a single phase angle (45°). The materials that have high diffuse directional hemispherical reflectance (DHR) values are trackable over the longest ranges. The metallic specular materials have shorter detection ranges at most of the lighting conditions that a probe would encounter in our design concept of operations.

Given the findings of this study, Beta Cloth[19] was selected as the preferred material. Beta Cloth is bright white, diffuse, radiation resistant, and has been used in many space applications, including astronaut suits. It consists of Teflon that is woven into a fabric, and its surface can be etched to improve its diffuse DHR. We tested samples and observed a roughly 85% albedo that is flat over visible wavelengths.
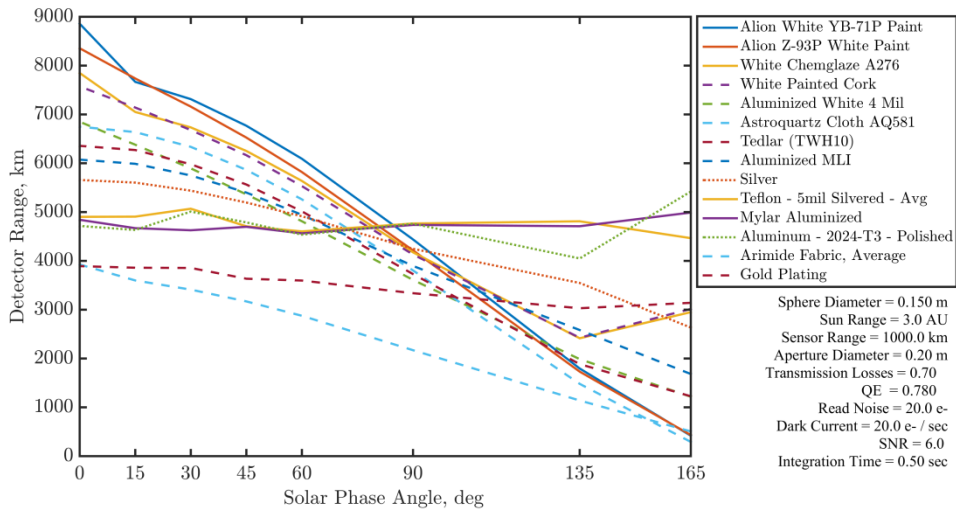
Figure 17. Simulated LORRI tracking range for a probe made of different materials.
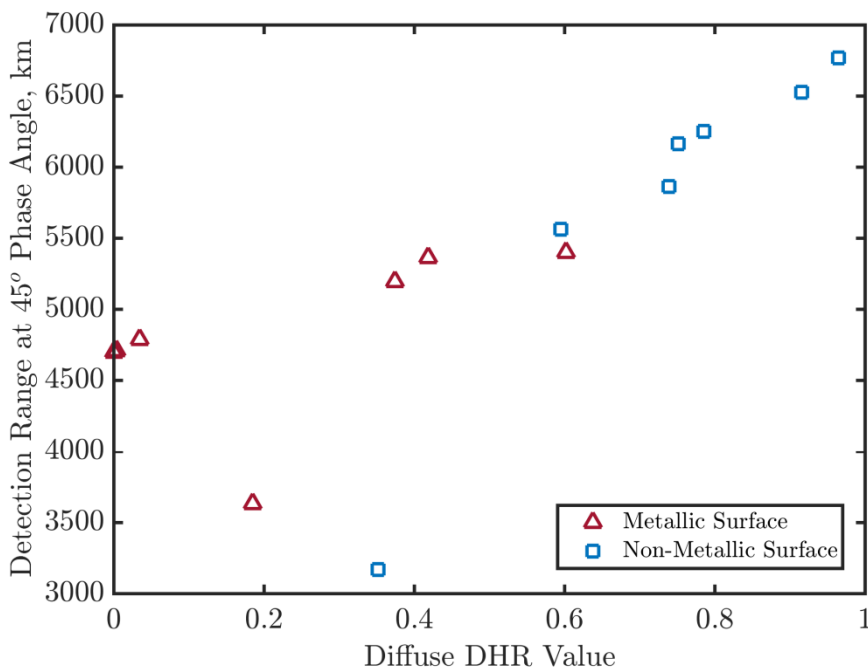

Figure 18. Simulated LORRI tracking range as a function of material, identified by diffusivity.

23

Figure 19. Probe sphere wrapped in sewn Beta cloth.

4.4   Dispenser Design

The dispenser functions to eject the probe into the intended trajectory at a velocity range of 3-5 m/s. The dispenser consists of a stack of multiple (4 shown) ejector assemblies, each containing an ejector release mechanism, a plunger, a pair of plunger preload mechanisms, and a linear compression spring sized appropriately to eject the sabot-probe assembly at the required velocity. The path of the plungers and sabots includes dovetails to ensure forward linear motion and prevent jamming. There is one door, shared by a set of ejector assemblies, that acts to contain the probes within the dispenser during launch. The door features a hinge, a release mechanism, and a tell-tale switch.

The stainless steel springs have been sized to work in a low shear stress state (less than 35% of shear stress to tensile stress) when stowed. This potentially mitigates the creep issue that occurs when the mechanism is left stowed for at least 5 years.

There are two pairs of LED emitters and detectors that measure the ejection velocity of each sabot-probe assembly. The sabot's ejection interrupts the light path between each pair of emitters and detectors. By reporting the time difference in these interruptions, we can determine the dispensed sabot velocity to better than a few mm/s.
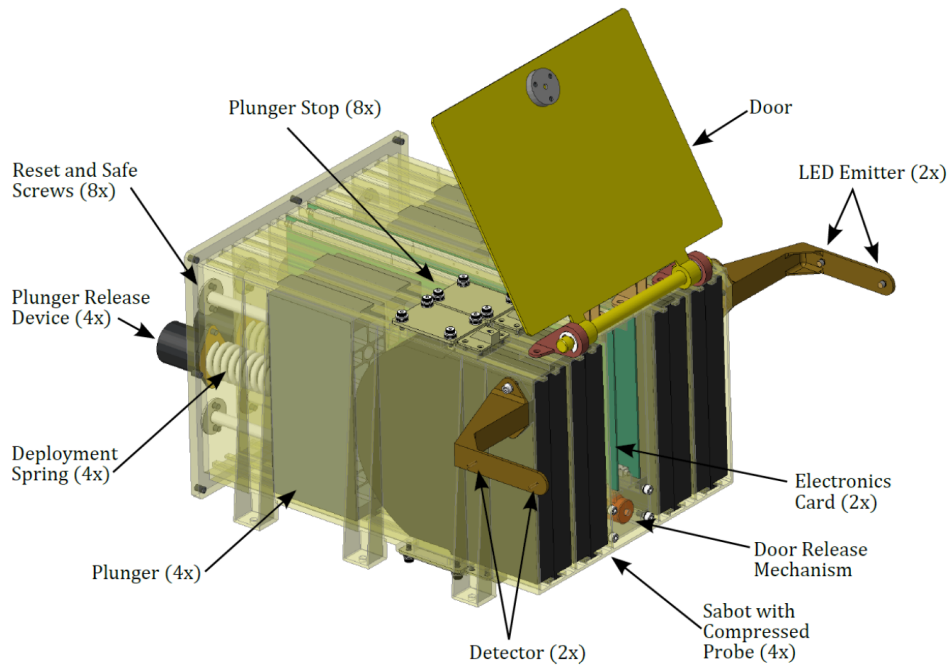
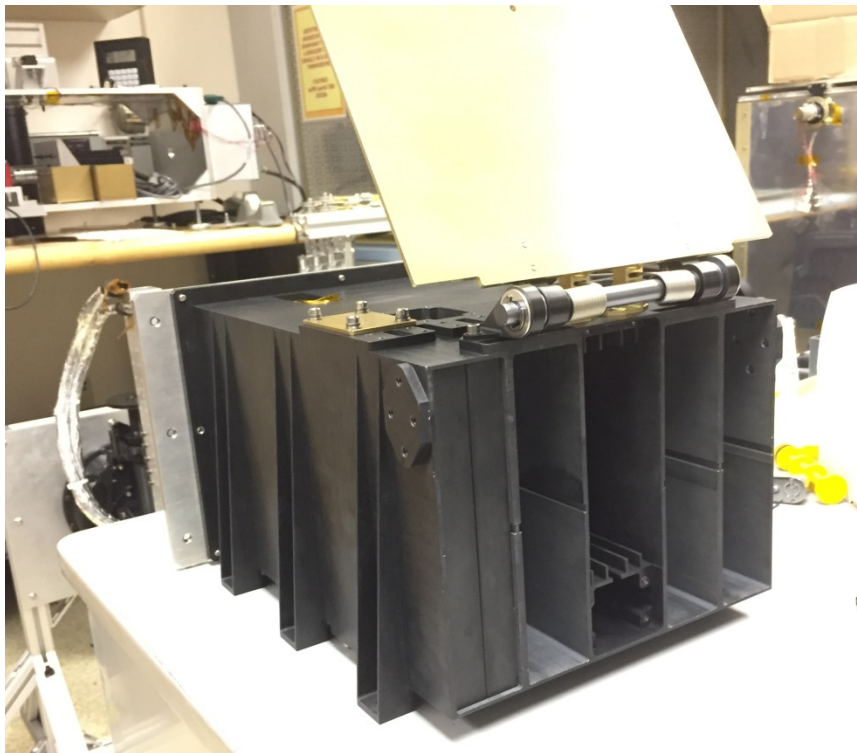Figure 20. Dispenser drawing with annotations.

Figure 21. Photo of dispenser with door open and one probe loaded at left. The door mechanism and optical measurement system are not yet attached.
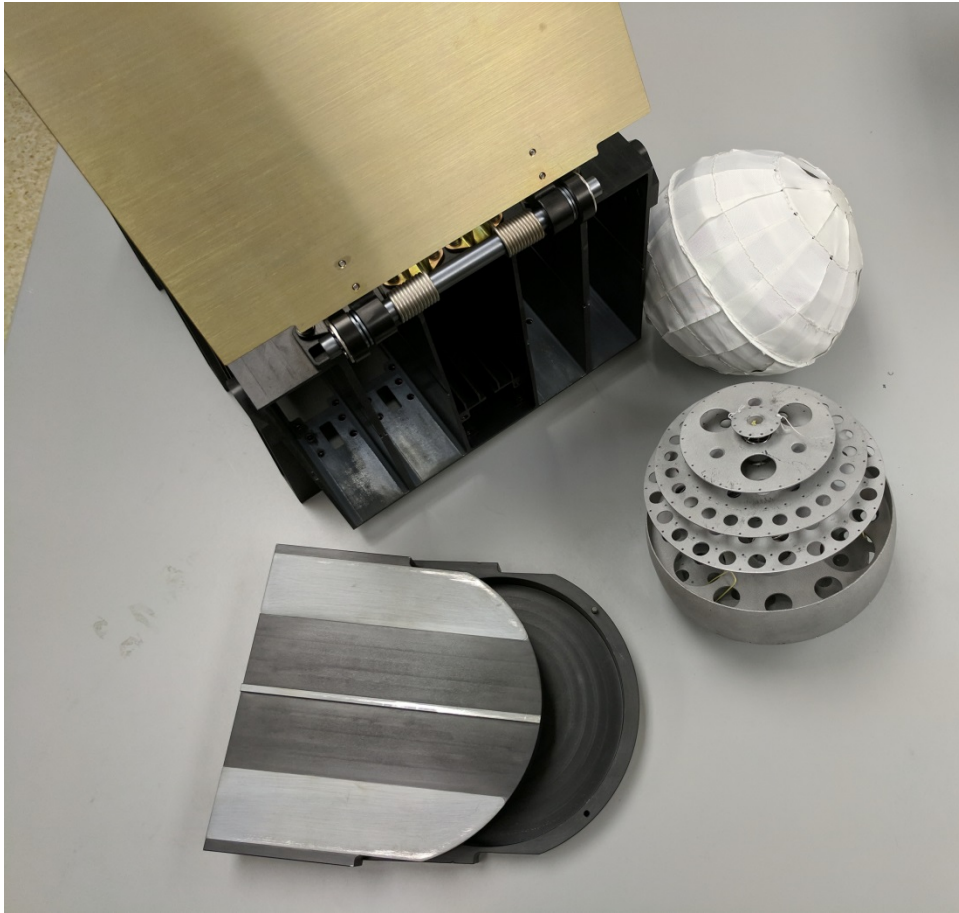
Figure 22. Photo of dispenser with door open, one covered probe, one uncovered probe, and two sabot halves.

4.5   Mass Summary

The as-measured mass values for the current prototype are given in Table 4. If electronics cards We anticipate being able to reduce this value up to 30% for future iterations based on lessons learned. There are also reductions possible if the design is customized for a particular mission. For example, the probe diameter could be reduced for operations near 1 AU.

Table 4. Measured Mass For Prototype

Component	Mass (kg)	Quantity	Total Mass (kg)
Probe & 2 Sabot Halves	1.18	4	4.72
Release Device, Spring, & Plunger	0.78	4	3.12
Empty Dispenser	8.68	1	8.68
Total			16.5

5 Testing

The completed prototype has undergone preliminary functional deployment testing. The intent was to verify operation and observe the dispenser and door-opening mechanism actuations using high-speed cameras.

5.1 Dispenser Testing

We test fired the dispenser twice with uncovered probes. Figure 23 shows six frames of the high speed video of one test taken from overhead. In this case, gravity is acting into the page. The uncovered probe is dispensed downward in the frame, with the sabot halves separating at right and left. Once the electronic release mechanism is fired, a compression spring expands and pushes the sabot assembly out of its chamber. When clear of the chamber, the uncovered probe expands quickly, pushing the sabot halves apart. The probe appears to have a slight clockwise angular velocity. This doesn't affect the performance, since the Beta cloth cover gives it a uniform response, independent of orientation.

5.2 Probe Release

We released a covered probe manually to observe the sphere's expansion with the resistance of Beta cloth. Five frames of the test are shown in Figure 24. In this case, the probe is ejected in the direction out-of-the-page, with gravity acting downward. The probe expanded easily, with the sabots separating and clearing the vicinity.

5.3 Door Release Opening

The door is released using a frangibolt. Once activated the door's hinge is opened using a set torsion springs. Figure 25 shows six frames of the high-speed video. Gravity is acting into the page, as the door opens counter-clockwise. The dispenser is observed recoiling as the door opens.
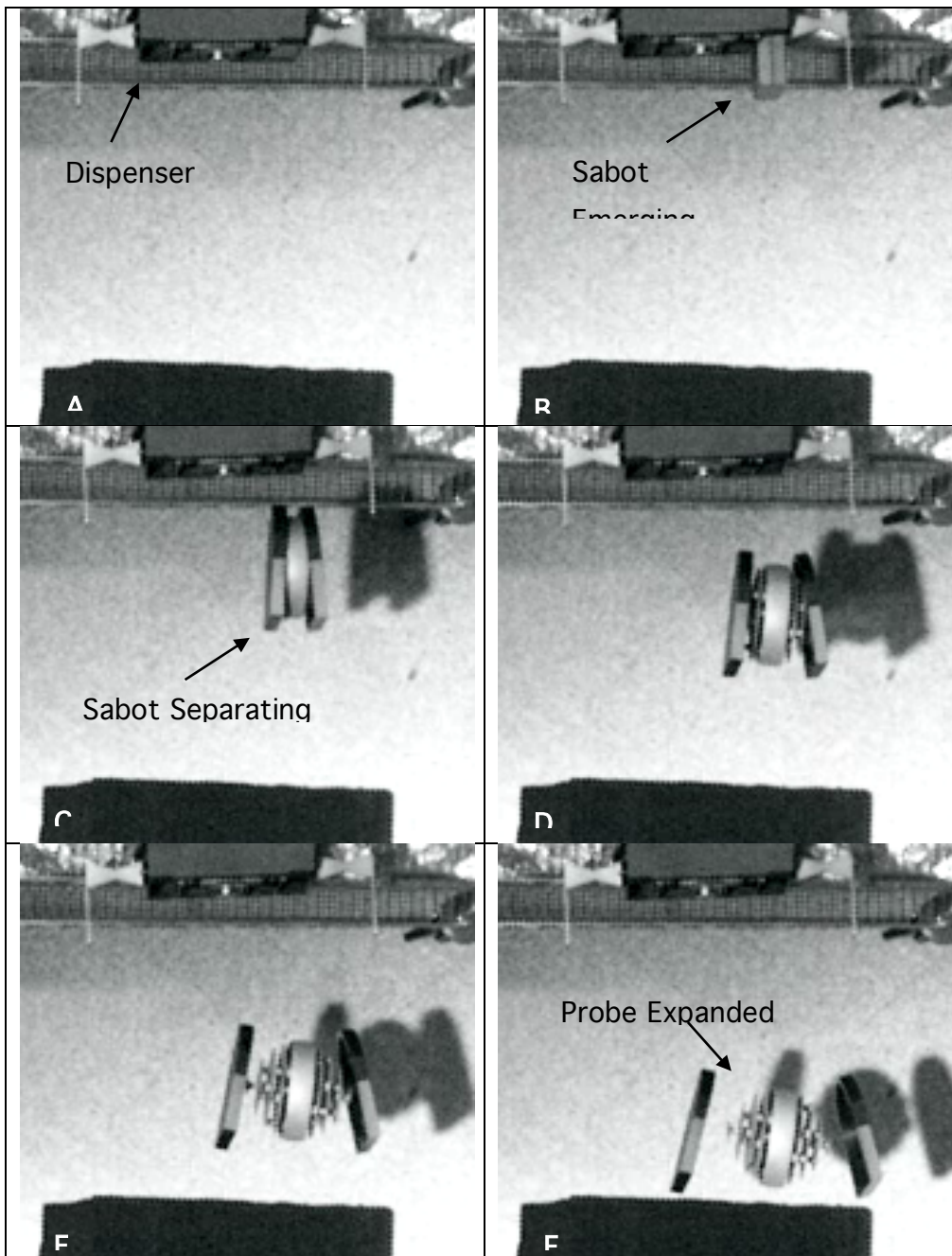
Figure 23. Probe Dispensing Process (A-F). Overhead view. The sabot and probe eject and separate, traveling downward.
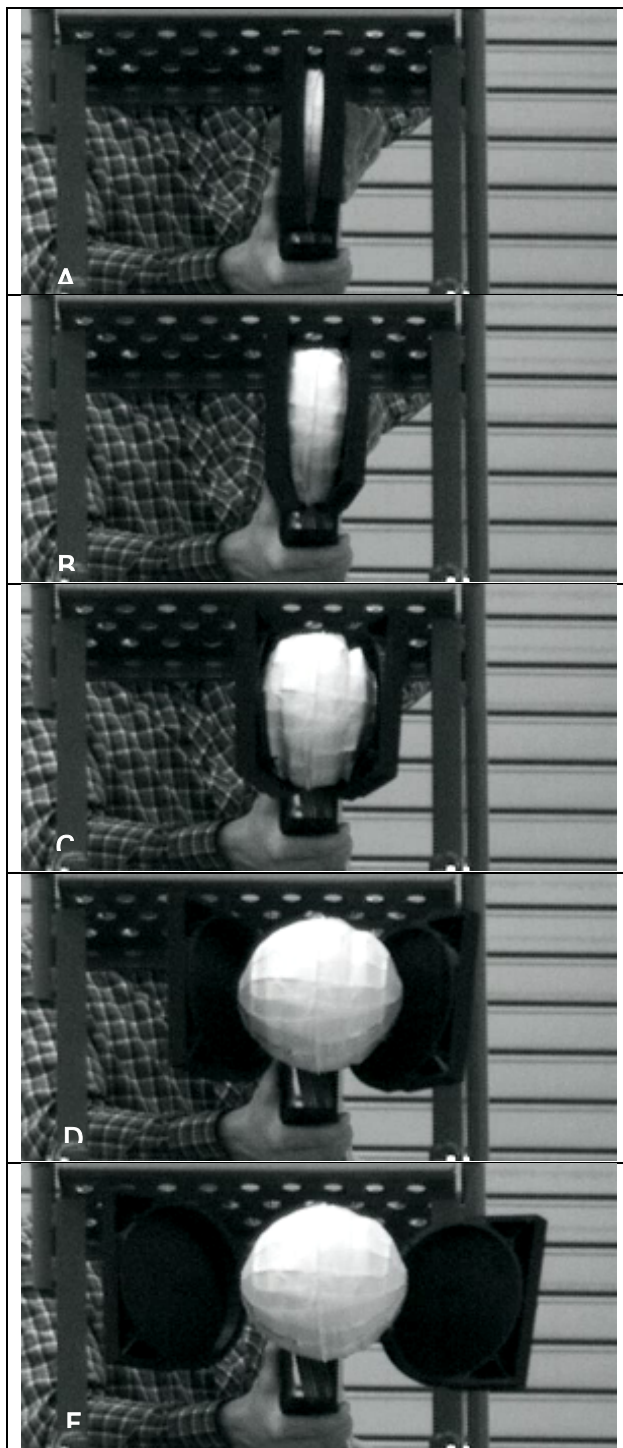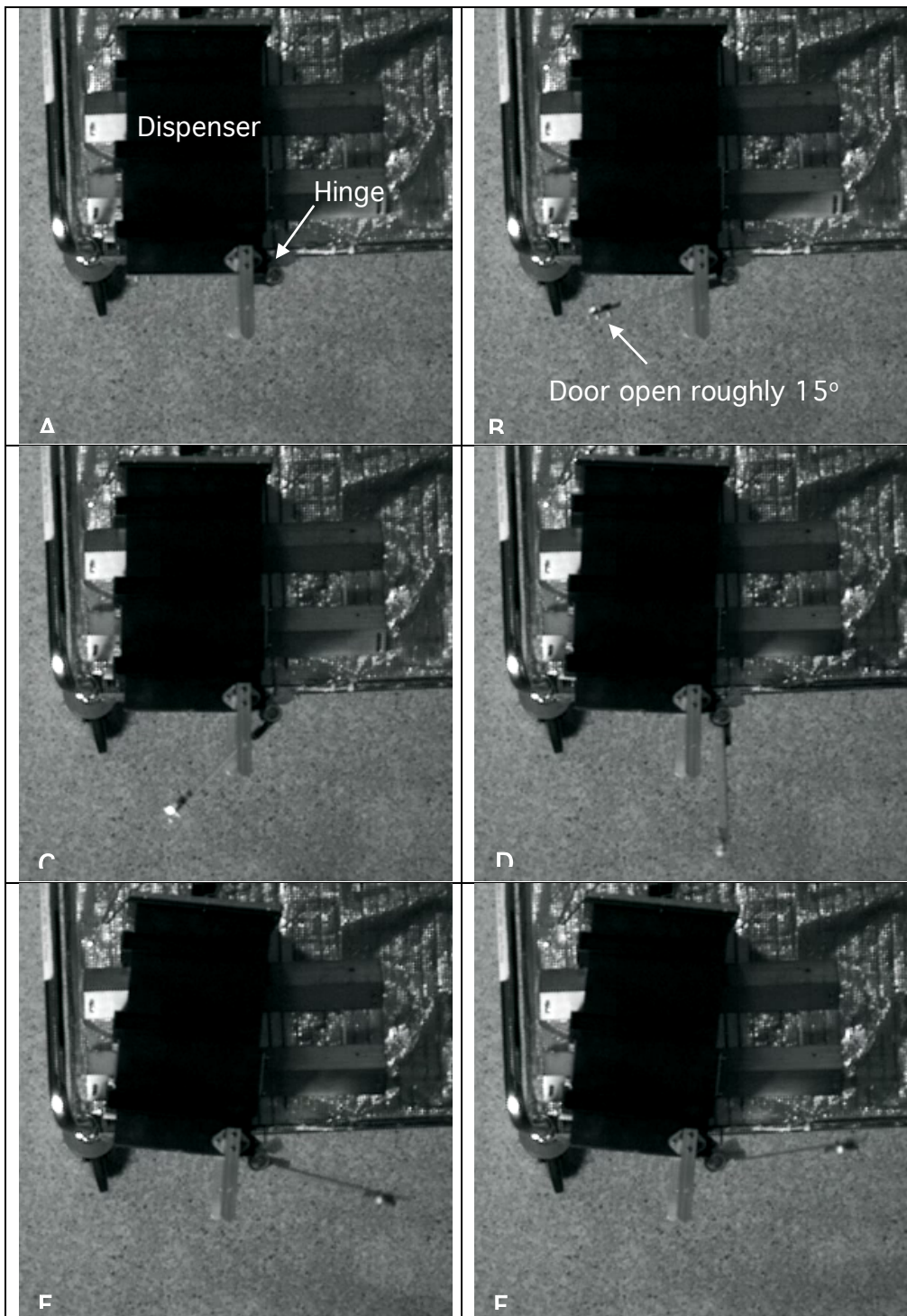
Figure 24. Covered Sphere Expansion (A-E).

Figure 25. Door Release Process (A-F). The dispenser recoils in reaction.

6 Next Steps

6.1 Hardware Maturity

The SIMMEE hardware has received preliminary functional testing. The next step is to subject it to further testing to characterize its deployment repeatability and accuracy. We also hope to subject the hardware to environmental tests to increase its technology readiness level. Ideally we intend to test the device at the NASA Glenn Research Center's Zero-G facility. Its 132 m long vacuum drop-tunnel would provide a very precise measurement of the deployment accuracy.

6.2 Extended Applications

We've studied OpGrav thoroughly in the context of asteroid flyby, where we believe it is most directly useful. However, we also hope to study OpGrav in the context of rendezvous operations. Preliminary simulations indicate that the test-masses can give very sensitive mass distribution measurements as compared to Earth-based Doppler only tracking. This would have implications for the speed and quality of gravity field estimation of the body, which reduces spacecraft risk and operations timelines. Figure 26 shows four concepts for how one might deploy a probe while rendezvoused to yield useful measurments.

6.3 Mission Implementation

Ultimately, we seek to implement this instrument on a planetary science mission. We believe that the most near-term means of doing so is participating with missions as a technology demonstration or via a student collaboration partner. Both means allow OpGrav to positively contribute to a mission with minimal investment. In the meantime, we will actively continue to pursue means of continuing its development and maturity.
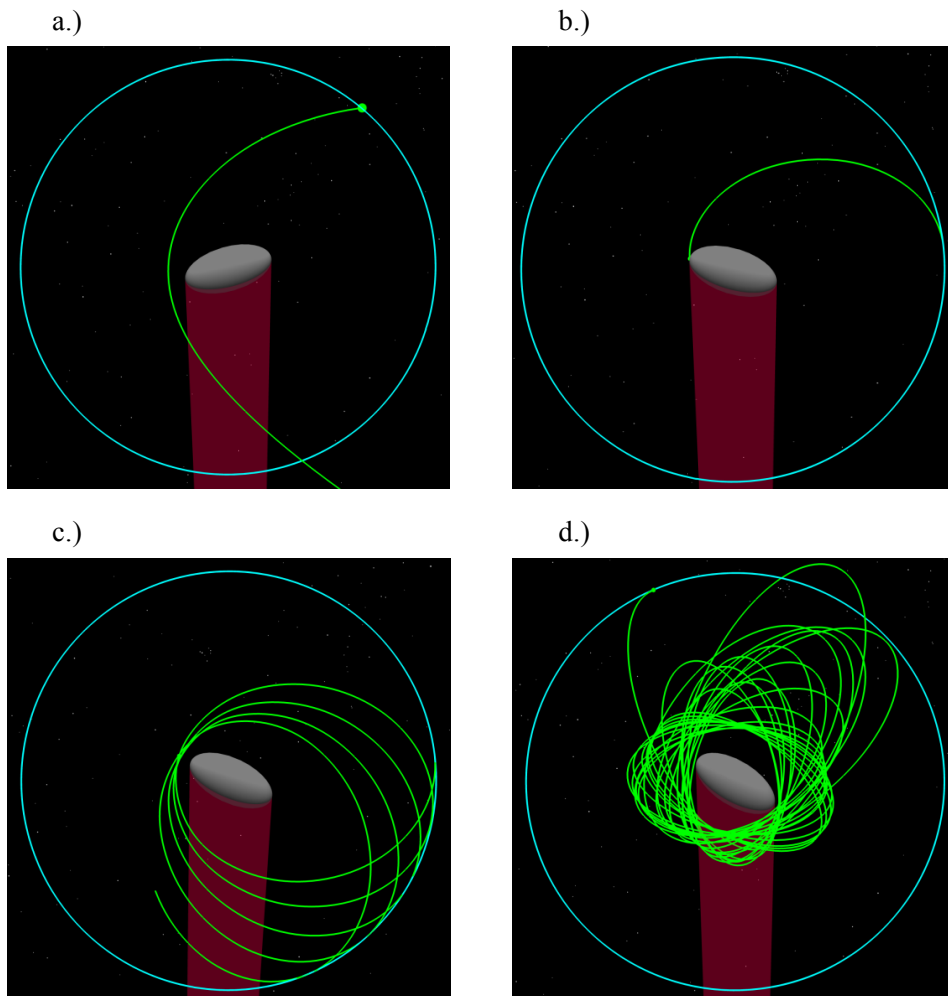
Figure 26. Four rendezvous deployment types illustrated: a.) Escape, b.) Impact, c.)Stable long-lived orbit, d.) Unstable orbit. In this simulation, the host spacecraft remains in a 50 km safe retrograde orbit (blue).

7 Acknowledgements

8   References

[1] G. Consolmagno, D. Britt, and R. Macke, "The significance of meteorite density and porosity," Chemie der Erde-Geochemistry, vol. 68, no. 1, pp. 1–29, 2008.

[2] M. B. Syal, J. M. Owen, and P. L. Miller, "Deflection by kinetic impact: sensitivity to asteroid properties," Icarus, vol. 269, pp. 50–61, 2016.

[3] B. Carry, "Density of asteroids," Planetary and Space Science, vol. 73, no. 1, pp. 98–118, 2012.

[4] J. A. Atchison and R. H. Mitch, "Asteroid flyby gravimetry via target tracking," AAS Spaceflight Mechanics Conference, Williamsburg VA, AAS-15-466, 2015.

[5] Tapley, B., Schutz, B., and Born, G., Statistical Orbit Determination, Elsevier Academic Press, Burlington, MA, 2004.

[6] A. F. Cheng, H. Weaver, S. Conrad, and et al., "Long range reconnaissance imager on new horizons," Space Science Reviews, vol. 140, pp. 189–215, October 2008.

[7] S. E. Hawkins III, S. L. Murchie, et al., "In-flight performance of messenger's mercury dual imaging system," in SPIE Optical Engineering + Applications. International Society for Optics and Photonics, 2009, pp. 74 410Z–74 410Z.

[8] H. Sierks, H. U. Keller, R. Jaumann, et al., "The dawn framing camera," Space Science Reviews, vol.163, no. 1, pp. 263–327, 2011.

[9] Marsh J. G., et al., "A new gravitational model for the Earth from satellite tracking data", Journal of Geophysical Research, Vol. 93, No. B6, 1988, 6169-6215.

[10] Mazarico E. M. Rowlands D. D., et al. "Orbit determination of the lunar reconnaissance orbiter", Journal of Geodesy, Vol. 86, No. 3, 2012, 193-207.

[11] Lemoine F G., et al., "An improved solution of the gravity field of Mars (GMM-2B) from Mars Global Surveyor", Journal of Geophysical Research, Vol. 106, E10, 23, 2001, 359-23, 376.

[12] Centinello F.J. III, et al., "Orbit determination of the Dawn spacecraft with radiometric and image data", Journal of Spacecraft & Rockets, Vol. 52, No. 5, 2015, 1331-1337

[13] J. A. Atchison, R. H. Mitch, E. Mazarico, "Optical Gravimetry for Flyby Missions: Parametric Study and Validation", Lunar and Planetary Science Conference, Houston, TX, 2017.

[14] R. H. Mitch, J. A. Atchison, A. S. Rivkin, "Optical Gravimetry – Implications for Planetary Defense", Planetary Defense Conference, Tokyo Japan, 2017.

[15] Harris A.W. et al. (2015) Icarus, pp 302-312

[16] R. H. Mitch, J. A. Atchison, A. S. Rivkin, "Simulated OpGrav Performance in a Main-Belt Asteroid Tour", Asteroids, Comets, Meteors, Montevideo Uraguay, 2017.

[17] A. S. Rivkin, R. Anderson, O. Barnouin, et al. "The Main-belt Asteroid and NEO Tour with Imaging and Spectroscopy (MANTIS)", IEEE Aerospace Conference, Big Sky MT, 2016.

[18] J. A. Atchison, R. H. Mitch, C. Apland, C. L. Kee, and K. W. Harclerode, "Small Body In-Situ Multi-Probe Mass Estimation Experiment (SIMMEE)", IEEE Aerospace Conference, Big Sky Montana, pp. 1-9, 2017

[19] S. L. Koontz, S. Jacobs, and J. Le, "Beta cloth durability assessment for space station freedom multi-layer insulation blanket covers," NASA Technical Report NASA-TM-104748, Mar 1993.